© 2019. Published by The Company of Biologists Ltd | Journal of Experimental Biology (2019) 222, jeb209015. doi:10.1242/jeb.209015

RESEARCH ARTICLE

Vision in the snapping shrimp *Alpheus heterochaelis*

Alexandra C. N. Kingston[1,*], Rebecca L. Lucia[1], Luke T. Havens[1,2], Thomas W. Cronin[3] and Daniel I. Speiser[1]

ABSTRACT

Snapping shrimp engage in heterospecific behavioral associations in which their partners, such as goby fish, help them avoid predators. It has been argued that snapping shrimp engage in these partnerships because their vision is impaired by their orbital hood, an extension of their carapace that covers their eyes. To examine this idea, we assessed the visual abilities of snapping shrimp. We found the big claw snapping shrimp, *Alpheus heterochaelis*, has spatial vision provided by compound eyes with reflecting superposition optics. These eyes view the world through an orbital hood that is 80–90% as transparent as seawater across visible wavelengths (400–700 nm). Through electroretinography and microspectrophotometry, we found the eyes of *A. heterochaelis* have a temporal sampling rate of >40 Hz and have at least two spectral classes of photoreceptors (λ_{max}=500 and 519 nm). From the results of optomotor behavioral experiments, we estimate the eyes of *A. heterochaelis* provide spatial vision with an angular resolution of ∼8 deg. We conclude that snapping shrimp have competent visual systems, suggesting the function and evolution of their behavioral associations should be re-assessed and that these animals may communicate visually with conspecifics and heterospecific partners.

KEY WORDS: Electroretinography, Microspectrophotometry, Optomotor, Orbital hood, Spectral sensitivity, Visual ecology

INTRODUCTION

The visual systems of animals vary in form and function, so different species may perceive similar surroundings in dissimilar ways. For example, the eyes of animals differ in how they resolve fine spatial details, distinguish between wavelengths of light, and perceive fast-moving objects or scenes (Land and Nilsson, 2012). Thus, characterizing the spatial acuity, spectral responses and temporal resolution of an animal's visual system will help identify visual cues that may influence the interactions of that animal with its environment (Caves et al., 2016; Cronin et al., 2014).

Asymmetries between visual abilities can influence the roles of species engaged in heterospecific behavioral associations. For example, both cleaner shrimp and the fish they clean tend to be brightly colored and boldly patterned, suggesting these partners assess color and pattern when choosing each other for cleaning interactions. However, an analysis of the visual abilities of cleaner shrimp indicates they are unable to distinguish the colors and patterns of conspecifics or clients; thus, fish may be using visual cues to choose their cleaners, but it is unlikely shrimp are using visual cues to choose their clients (Caves et al., 2016).

Similarly, asymmetries between visual abilities may influence behavioral associations between some species of snapping shrimp (Decapoda: Alpheidae; also known as pistol shrimp; Fig. 1A) and heterospecific partners such as gobies (Perciformes: Gobiidae) (Karplus, 1987; Karplus and Thompson, 2011; Luther, 1958; Magnus, 1967; Preston, 1978). Snapping shrimp are well known for their ability to produce cavitation bubbles with their specialized snapping claws. When these cavitation bubbles collapse, they release energy in the form of sound, light and a shock wave that can stun or kill potential predators or prey (Knowlton and Moulton, 1963; Lohse et al., 2001; Versluis et al., 2000). Another unique feature of snapping shrimp is their orbital hood, which is an extension of the carapace that covers their eyes (Anker et al., 2006). It has been hypothesized that these orbital hoods impair vision in snapping shrimp, perhaps even rendering them blind (Luther, 1958; Magnus, 1967). To explain the behavioral associations observed between them, it has been argued that gobies act as lookouts for snapping shrimp by monitoring the environment for predators (Magnus, 1967). In return, it is thought that snapping shrimp provide shelter for their goby partners by digging and maintaining shared burrows (Karplus, 1987).

A complication to our current understanding of heterospecific partnerships involving snapping shrimp is that snapping shrimp may be able to see. We hypothesize that snapping shrimp have spatial vision for several reasons: first, snapping shrimp have compound eyes beneath their orbital hood (Fig. 1B,C); second, the orbital hood appears to be highly transparent (Fig. 1B); and third, behavioral evidence suggests that snapping shrimp use visual cues to assess conspecifics during agonistic interactions (Hughes, 1996a, b). If snapping shrimp are able to see, we will have to re-evaluate why some species establish heterospecific partnerships. Further, having competent vision would introduce the possibility that snapping shrimp might use visual cues to communicate with conspecifics and heterospecific partners.

To better understand the visual ecology of snapping shrimp, as well as the function and evolution of their heterospecific partnerships, we assessed the visual abilities of the big claw snapping shrimp *Alpheus heterochaelis* Say 1818 (Fig. 1A). To do so, we examined the morphology of the eyes, measured the optical properties of the orbital hood using transmission spectroscopy, assessed the temporal and spectral responses of the eyes using electroretinography (ERG) and microspectrophotometry (MSP), and estimated spatial resolution using optomotor behavioral assays.

MATERIALS AND METHODS

Animal collection and care

We collected specimens of *A. heterochaelis* from two sites in North Inlet Estuary: Oyster Landing (33°20′58.5″N, 79°11′19.2″W) and Clambank Creek (33°20′03.7″N, 79°11′32.7″W). We collected animals from oyster beds during daytime low tides, at depths of less than 1 m, using hand nets on 10 July 2017, 7–9 August 2017 and

[1]Department of Biological Sciences, University of South Carolina, Columbia, SC 29208, USA. [2]Department of Biology, University of North Carolina, Chapel Hill, NC 27599, USA. [3]Department of Biological Sciences, University of Maryland Baltimore County, Baltimore, MD 21250, USA.

*Author for correspondence (kingstoa@mailbox.sc.edu)

A.C.N.K., 0000-0002-1982-8831; T.W.C., 0000-0002-2643-0979; D.I.S., 0000-0001-6662-3583

Received 17 June 2019; Accepted 7 October 2019

Journal of Experimental Biology (2019) 222, jeb209015. doi:10.1242/jeb.209015

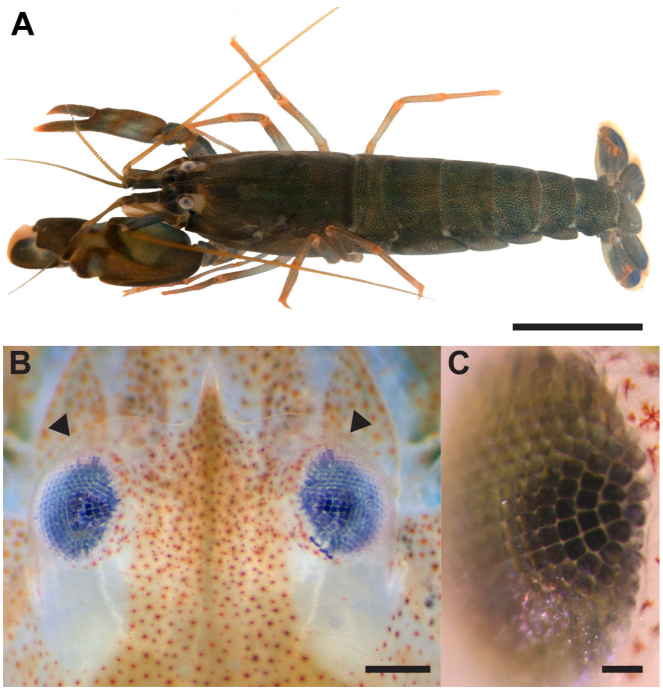

Fig. 1. *Alpheus heterochaelis*, the big claw snapping shrimp. (A) Image of *A. heterochaelis*. Scale bar: 1 cm. (B) The eyes of *A. heterochaelis* are covered by the orbital hood (arrowheads mark the anterior margin of the orbital hood). Scale bar: 500 µm. (C) Close up of the square facets of the reflecting superposition eye of *A. heterochaelis*. Scale bar: 50 µm.

18 June 2018. After collection, we held animals in natural seawater (NSW) in individual containers on a shaded outdoor porch. Within 5 days of collecting animals, we fixed them for morphological examination, used them for transmittance measurements or transported them to the University of South Carolina (Columbia, SC, USA) for physiological and behavioral experiments. At the University of South Carolina, we held animals communally in a 227 l tank filled with NSW at room temperature (~22–23°C), a salinity of 35 ppt and a 12 h:12 h light:dark cycle in which light was provided by two 24-inch TrueLumen Pro LED fixtures (Current USA, Vista, CA, USA). We fed animals twice per week with Hikari Crab Cuisine (Kyorin Food Ind. Ltd, Himeji, Japan).

Eye morphology

To examine eye morphology in *A. heterochaelis*, we fixed whole specimens in 2.5% methanol-free paraformaldehyde (Electron Microscopy Sciences, Hatfield, PA, USA) plus 2.5% glutaraldehyde (Polysciences, Inc., Warrington, PA, USA) in 0.22 µm filtered NSW for either 4 h at room temperature or overnight at 4°C. After fixation, we stored animals in 0.1 mol l^{-1} phosphate-buffered saline (PBS) at 4°C until use.

To image intact eyes from fixed specimens (n=6 individuals), we used an M165FC stereomicroscope and a DFC295 digital microscope camera (Leica Microsystems, Buffalo Grove, IL, USA). To calibrate the images, we used an ocular micrometer. From the images, we used the open-source software Fiji (Schindelin et al., 2012) to measure the diameter of eyes and individual facets, and to estimate the number of facets per eye. We used Fiji and the Kappa plugin (Bechstedt et al., 2014) to calculate the radius of curvature of the eyes.

To image sectioned eyes, we dissected eyes from fixed specimens and prepared them for cryosectioning by incubating them overnight at 4°C in a graded series of sucrose solutions at concentrations of 10%, 20% and 30% in PBS. Using a Leica CM1850 cryostat set to −20°C, we cut 10 µm sections onto SuperFrost Plus slides (Fisher, St Clair Shores, MI, USA). We acquired transmitted light images of sections using a Leica TCS SP8 X confocal microscope and a water-immersion Leica 40× objective (NA 1.10).

Optical properties of the orbital hood

We measured the transmission of light through the orbital hoods of *A. heterochaelis* using a modified Olympus CX-31 microscope (Center Valley, PA, USA). We removed the lamp and condenser from this microscope and replaced the right eyepiece with a custom-made SMA adapter. To the adapter, we affixed an optical fiber (QP400-1-UV-VIS; Ocean Optics, Dunedin, FL, USA) that supplied light from a 20 W tungsten-halogen lamp (HL-2000-HP-FHSA; Ocean Optics). Using an Olympus 10× PlanC N UIS2 objective, we focused light from the lamp into a spot 0.3 mm wide at the level of the microscope stage. Below the stage, light was refocused by a mounted biconvex lens (LB1761-A-ML: ThorLabs, Newton, NJ, USA) onto the end of an optical fiber (QP400-1-UV-VIS; Ocean Optics). We attached the biconvex lens to the condenser ring and positioned the end of the optical fiber at the focal point of the lens using an SMA adapter and a 30 mm lens tube (SM1L15; ThorLabs). Light transmitted by the optical fiber traveled to a Flame-S-VIS-NIR-ES spectrometer that we operated using Ocean View software (Ocean Optics).

For each specimen, we removed the orbital hood and split it into right and left halves along the rostrum. From each animal, we also removed a piece of pigmented carapace from a region immediately posterior to the orbital hood. We mounted these pieces of carapace in NSW between two coverslips (No. 1.5; Corning, New York, NY, USA). Using NSW as a reference, we measured the transmittance of tissue samples (400–700 nm) within 5 min of removing them from specimens. We then used one-way ANOVA to compare the transmittance values of the right and left sides of the orbital hoods and the pieces of pigmented carapace (n=40 individuals for each tissue type).

We estimated the refractive index of the orbital hood of *A. heterochaelis* using a set of refractive index liquids (Series E, Cargill Laboratories, Cedar Grove, NJ, USA). To do so, we anesthetized shrimp (n=8) in ice-cold NSW and removed their hoods. We dried each hood with a Kimwipe (Kimberly-Clark, Dallas, TX, USA) then placed it in 100 µl of a refractive index liquid (index of refraction n_d=1.51, 1.52, 1.53 or 1.54). We chose to evaluate refractive indices within this range because previous studies estimated the refractive index of crustacean carapace to be $n_d \approx 1.525$ (Becking and Chamberlin, 1925). We scored an orbital hood as matching a refractive index liquid when the tissue was invisible in the liquid.

ERG

Equipment

We used ERG to assess the temporal and spectral responses of the eyes of *A. heterochaelis*. We amplified DC signals using an A-M Systems model 3000 AC/DC differential amplifier with headstage (Sequim, WA, USA) set to a low-pass cut-off frequency of 20 kHz, digitized signals using a ADInstruments PowerLab model 8/35 data acquisition board (Colorado Springs, CO, USA) and compared signals using LabChart 8 Pro (ADInstruments). We dampened electromagnetic and vibrational noise by taking recordings inside a custom-built Faraday cage that was set atop a passively isolated air table with an attached breadboard (ThorLabs SDH7512 and

B3048F). As electrodes, we used electrolytically sharpened 0.2 mm tungsten rods (A-M Systems). We placed these electrodes using Narishige MM-3 manual micromanipulators (Amityville, NY, USA).

For test stimuli, we generated broad-spectrum light with a Spectral Products 150 W tungsten-halogen lamp (ASBN-W150-PV; Putnam, CT, USA) and then controlled the wavelength, intensity and temporal dynamics of this light using, respectively, a Spectral Products CM110 monochromator with a slit width of 1.2 mm; a continuously variable, circular neutral density filter (Edmund Optics 54-082; Barrington, NJ, USA); and a Uniblitz LS3 high-speed shutter (Rochester, NY, USA). For adapting stimuli, we produced and controlled light with a 20 W tungsten-halogen lamp with an integrated shutter (Ocean Optics HL-2000-HP-FHSA); a 520 bandpass filter (Thorlabs FB520-10); and a continuously variable, circular neutral density filter (Edmund Optics 54-082).

To prepare animals for ERG, we chilled them in NSW on ice. Next, to prevent animals from desiccating, we wrapped them in a Kimwipe that had been soaked in chilled NSW. We then attached animals to a nylon post by wrapping them in Parafilm (Bemis Company, Inc., Oshkosh, WI, USA). Before placing the recording electrode, we made a small incision through a specimen's orbital hood and right eye using a 26G needle. For every trial, we placed the recording electrode in an animal's right eye. We performed monopolar recordings by electrically coupling ground and reference inputs to a single electrode placed in the dorsal thorax.

We quantified the absolute spectral irradiance (integrated from 375 to 725 nm) of the test and adapting stimuli at a distance and orientation similar to those of the preparations. To do so, we used a spectrometer system with components from Ocean Optics that included a Flame-S-VIS-NIR-ES spectrometer, a QP400-1-UV-VIS optical fiber and a CC-3 cosine corrector. To calibrate the absolute spectral response of the spectrometer, we used an HL-3P-CAL Vis-NIR calibrated light source. We operated the system using Ocean View software.

Spectral responses

To assess the spectral responses of the eyes *A. heterochaelis*, we measured the variation in their electrophysiological response magnitudes to isoquantal stimuli of differing wavelengths. We performed four trials on each specimen of *A. heterochaelis* (n=12, 6 males and 6 females): in two of the four trials, we maintained animals in a state of dark adaptation; in the other two trials, we maintained a state of light adaptation. We presented these trials in a pattern of dark–light–dark–light and began each trial with an initial adaptation period lasting 15 min. We chose 15 min adaptation periods to maximize the time test animals spent under each adapting condition while minimizing the duration of each trial, a concern for us because snapping shrimp tended to die in preliminary trials lasting longer than 2 h. In the light-adaptation trials, we filtered broadband light through a 520 nm bandpass filter (ThorLabs) with a full width at half maximum (FWHM) of 10 nm and presented it at an intensity of 1.92×10^{15} photons cm^{-2} s^{-1}. Here, our goal was to use the adapting light to reveal photoreceptors whose activities may have been masked by the strong responses of photoreceptors with spectral peaks ∼500 nm.

In each trial, we presented 31 monochromatic, intensity-balanced test stimuli in random order every 10 nm from 400 to 700 nm. All of these stimuli were presented within 10% of the goal intensity of 1.92×10^{14} photons cm^{-2} s^{-1}. From preliminary trials, the stimulus intensity of 1.92×10^{14} photons cm^{-2} s^{-1} elicited responses from test animals across the visible spectrum without saturating the response at any wavelength. We presented these test stimuli for 1 s with a 10 s off period immediately following each stimulus. In the dark-adaption trials, there was no light during this 10 s off period. In the light-adaptation trials, the adapting light remained on during both presentation of the test stimuli and the off period.

We assessed the responses of the eyes of *A. heterochaelis* to light of different wavelengths by measuring the maximum deflection from resting voltage associated with the presentation of each test stimulus. We had two technical replicates for each type of trial (dark adapted or light adapted). We averaged together the responses of animals to the same wavelength in the same type of trial to produce a mean response for every animal to each condition and wavelength. To compare between animals, we normalized their responses, with each animal's response of greatest magnitude scored as one and their response of lowest magnitude scored as zero.

Temporal resolution

To assess the temporal responses of the eyes of *A. heterochaelis* (n=8, 4 males and 4 females), we used ERG to test their flicker fusion frequency (FFF) to a monochromatic, 500 nm light stimulus with an intensity of 7.89×10^{14} photons cm^{-2} s^{-1}. We chose to assess FFF in *A. heterochaelis* at 500 nm because preliminary trials indicated that this is their wavelength of peak spectral response. We used an intensity of 7.89×10^{14} photons cm^{-2} s^{-1} because it was the brightest 500 nm stimulus that we could produce with our system configuration. Before testing them, we dark adapted animals for 15 min. Each set of recordings consisted of a series of light stimuli flickering at rates of 10–49 Hz in steps of 1 Hz. Each stimulus flickered for 3 s and was then followed by 3 s of darkness. We scored an animal as following a stimulus if its response peaks matched the flickering stimulus for at least 10 flashes in a row.

MSP

We used MSP to measure the spectral absorbance of photoreceptors from the eyes of *A. heterochaelis*. We recorded from specimens within 10 days of collection from the field. Prior to MSP recordings, we dark adapted animals for a minimum of 16 h. We performed all subsequent procedures in the dark or under dim red light. After dark adapting a specimen, we removed its head and then the orbital hood from the head. We mounted each head in Tissue-Tek O.C.T. Compound (Sakura Finetek USA Inc., Torrance, CA, USA) on a metal stub, flash froze the sample, and then placed the stub in an IEC cryomicrotome (International Equipment Co., Boston, MA, USA) held at −20°C. Using the cryomicrotome, we cut 12 µm thick sections from heads, and then mounted sections within a ring of silicone grease between coverslips in a Ringer's solution for marine crustaceans with 1% glutaraldehyde added.

We performed MSP on sections using methods and equipment described previously (Cronin and Forward, 1988; Cronin and Marshall, 1989; Cronin et al., 2002). Using a single-beam microspectrophotometer, we scanned transverse and oblique sections of rhabdoms in steps of 1 nm across a wavelength range of 400–700 nm, with the monochromator advancing from short to long wavelengths. We made sure to take measurements from regions of photoreceptors where the MSP beam passed through little or no screening pigment. For reference values, we scanned areas of preparations that lacked tissue.

To record from dark-adapted photoreceptors, we took 'dark' scans by placing the beam in a rhabdom and initializing a scan. To record from photoreceptors with bleached visual pigments, we took 'white light' scans after exposing rhabdoms to 2 min of white light produced by the substage illuminator of the microscope. We scanned 76 rhabdoms from n=6 individuals (3 males, 3 females). For each of

Journal of Experimental Biology (2019) 222, jeb209015. doi:10.1242/jeb.209015

these rhabdoms, we acquired a dark scan and a white light scan. For some rhabdoms, we acquired a second white light scan.

To analyze MSP scans, we subtracted white light scans from dark scans to produce difference spectra for each photoreceptor. We then fitted the resulting difference spectra to a rhodopsin template (Govardovskii et al., 2000) using a least-squares procedure (Cronin et al., 2002; Frank et al., 2012).

Optomotor trials

We estimated spatial resolution in *A. heterochaelis* using optomotor response assays, a well-established method for assessing the visual abilities of decapod crustaceans and other animals (Baldwin and Johnsen, 2011; Caves et al., 2016; Hathaway and Dudycha, 2018; McCann and MacGinitie, 1965). In these assays, the visual abilities of animals are assessed through observations of their responses to rotating gratings of vertical stripes with different angular widths.

To conduct optomotor assays on snapping shrimp, we mounted stimuli to a rotating cylinder with a 30 cm diameter. We rotated the 30 cm cylinder using a bipolar high torque stepper motor (OMC Corporation Limited, Nanjing City, China) operated by an Arduino Uno microcontroller with an attached motor shield (Adafruit, New York, NY, USA). The 30 cm cylinder rotated around a stationary cylinder with a 25 cm diameter. We filled the 25 cm cylinder with NSW to minimize the amount of air through which the animals viewed the stimuli. In the center of the 25 cm cylinder, we placed animals in an NSW-filled cylinder with a 7.5 cm diameter. We did so to ensure that the angular widths of the stimuli, as viewed by the shrimp, remained as we intended.

We illuminated the optomotor apparatus from above using a single, centrally mounted Aqua Illumination Prime HD LED fixture (C2 Development, Inc., Ames, IA, USA; output 400–700 nm) whose broad-spectrum light we diffused with two filters mounted in series (3000 Tough Rolux and 3027 Half Tough White Diffusion; Rosco Laboratories, Stamford, CT, USA). Using the spectrometer system described above, we found that the absolute spectral irradiance of the downwelling light in the optomotor set-up was 1.85×10^{15} photons cm^{-2} s^{-1} at the position of the test animals. We recorded the optomotor trials using a GoPro Hero 6 (GoPro Inc., San Mateo, CA, USA).

We tested the optomotor responses of *A. heterochaelis* to black stripes printed on white paper that had angular widths of 20, 15, 12, 10, 8, 4, 2, 1 or 0.5 deg. For each stimulus, all of the black and white stripes were the same width. Every trial lasted 2 min, with the stripes rotating clockwise for 1 min and then rotating counterclockwise for 1 min. In every trial, the stripes completed 6 rotations per minute, a speed we found to be effective in preliminary trials. In the first set of trials, we tested the responses of 33 animals to rotating stripes with angular widths of 20, 15 or 10 deg. In the second set of trials, we tested the responses of 23 animals to stripes with angular widths of 12, 8 or 4 deg. In the third set of trials, we tested the responses of 30 animals to stripes with angular widths of 4, 2, 1 or 0.5 deg. In all sets of trials, we tested the responses of each animal to every stimulus, as well as a control stimulus that was a uniform 50% gray. We presented these stimuli in a random order to each animal and we tested an animal's response to one stimulus per day.

We assessed the responses of animals to optomotor stimuli from video (e.g. Movie 1). We considered an animal to be responding to a stimulus if it moved in the same rotational direction as the stimulus at approximately the same angular speed for at least 180 deg. We determined that an animal was able to follow a stimulus of a particular angular width if it met our criteria for responding to the stimulus in both clockwise and counterclockwise directions. In our trials, this consisted of an animal responding to a stimulus, the stimulus changing direction, and then the animal changing direction to respond to the new direction of the stimulus.

We analyzed the results of these trials by using a two-tailed Fisher's exact test to compare the ratio of animals that followed each set of stripes to the ratio of animals that followed the control stimulus. To account for multiple comparisons in the first two trials (three treatments compared back with one control in each trial), we applied a Bonferroni correction for multiple tests that specified the P-values had to be $P<0.0167$ and $P<0.0033$ to be significant at the levels of $P<0.05$ and $P<0.01$, respectively. To account for multiple comparisons in the third set of trials (four treatments compared back with one control), we applied a Bonferroni correction for multiple tests that specified that the P-values had to be $P<0.01$ to be significant at the level of $P<0.05$.

RESULTS

Snapping shrimp have reflecting superposition eyes

We found that snapping shrimp have compound eyes with reflecting superposition optics. Each facet in the eye of *A. heterochaelis* has a crystalline cone composed of four cells (Fig. 2), similar to what is observed in other crustaceans (Melzer et al., 1997). These facets are square in shape (Fig. 1C), similar to facets from the reflecting superposition eyes of other decapods and dissimilar to facets from compound eyes with apposition or refracting superposition optics (Land and Nilsson, 2012). Each main rhabdom in the eye of *A. heterochaelis* is composed of seven retinular cells (Fig. 2), again as expected for an eye from a decapod. We did not observe R8 cells distal to the main rhabdoms, but further examination will be necessary to verify the presence or absence of these photoreceptors, which are often UV sensitive in crustaceans (Cronin et al., 2014). Unlike the eyes of most decapods, those of *A. heterochaelis* are not stalked. They are also relatively soft, having a pliancy similar to eyes from other decapods (such as crayfish) immediately following a molt.

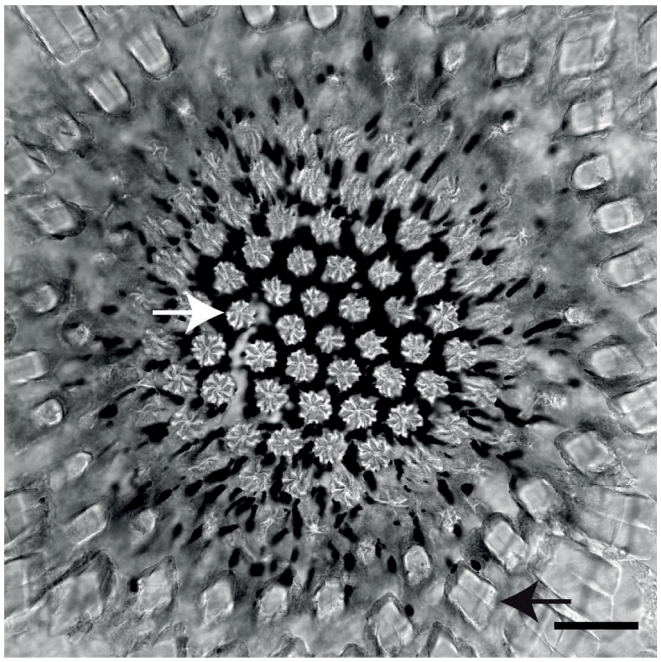

Fig. 2. Cross-section of the retina of *A. heterochaelis*. The white arrow points to a main rhabdom, composed of seven retinular cells. The black arrow points to a crystalline cone, composed of four square cells. Scale bar: 50 µm.

Journal of Experimental Biology (2019) 222, jeb209015. doi:10.1242/jeb.209015

We estimated that adjacent ommatidia from the eyes of *A. heterochaelis* are separated by angles of 6 deg ($\Delta\phi$). The eyes of *A. heterochaelis* are hemispherical in shape with a diameter of 880±42 µm and a radius of curvature of 293±39 µm (mean±s.d.; n=6 eyes from 6 separate individuals, each ∼3 cm in length). The facets of these eyes are 31±3 µm in diameter (n=18, with 3 facets measured per eye from 6 individuals). We counted 24±1 facets along the sagittal and transverse midlines of each eye (n=6 eyes from 6 separate individuals). These facets are similar in size and shape across the surfaces of the eyes and are packed contiguously. Thus, we estimated $\Delta\phi$ for *A. heterochaelis* by dividing facet diameter by the radius of curvature of each eye. The angular resolution of a compound eye is best described by the acceptance angles of its ommatidia ($\Delta\rho$), but in many species $\Delta\rho$ and $\Delta\phi$ are similar (Cronin et al., 2014; Land and Nilsson, 2012).

The orbital hoods of snapping shrimp are highly transparent

The orbital hoods of *A. heterochaelis* cover the eyes and are continuous with the surrounding carapace except along their anterior–ventral margin. Unlike the surrounding carapace, the orbital hoods lack pigmentation (Fig. 1B). Using transmission spectroscopy (Fig. 3), we found the orbital hoods of *A. heterochaelis* are highly transparent: relative to seawater, they transmit 80–90% of visible wavelengths (400–700 nm). In comparison, the surrounding carapace transmits 30–70% of visible wavelengths. Using one-way ANOVA, we found the transparencies of the left and right sides of the orbital hoods did not differ, but that both sides of the orbital hood were more transparent than the surrounding carapace (P<0.01 for comparisons of both sides of the orbital hood with the surrounding carapace; n=40 for all tissues types). Using index matching liquids, we found the orbital hoods of *A. heterochaelis* have a refractive index of ∼1.52, similar to the surrounding carapace and to previous estimates for the chitin-based exoskeletons of crustaceans (Becking and Chamberlin, 1925).

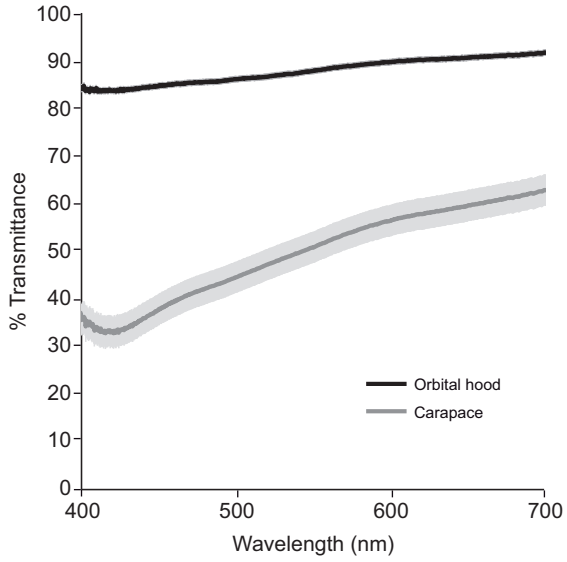

Fig. 3. Transmittance of light (400–700 nm) through the orbital hood and surrounding carapace of *A. heterochaelis*. Orbital hood, n=80; carapace, n=40. Shading represents ±2 s.e. from the mean. Transmittance values from the left and right orbital hoods were pooled because they did not differ statistically.

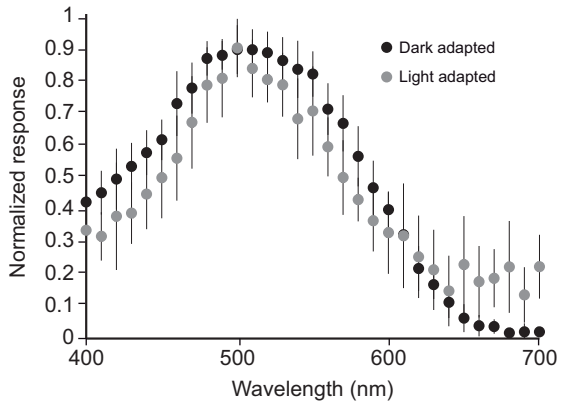

Fig. 4. Spectral responses of the eyes of *A. heterochaelis* assessed by extracellular electroretinography (ERG). Recordings from dark-adapted eyes are shown in black. Recordings from eyes that were light adapted using a 520 nm bandpass filter are shown in gray. Data points represent averages of responses normalized for each individual (n=12). Error bars represent ±1 s.d. from the mean.

Snapping shrimp are maximally sensitive to blue–green light

ERG and MSP indicated the eyes of *A. heterochaelis* detect light using at least two middle wavelength-sensitive (MWS) photoreceptors. Using ERG, we found dark-adapted eyes responded maximally to 500 nm light; after adapting eyes with 520 nm light, we found they again demonstrated a maximal response to 500 nm light (Fig. 4; n=12 for both conditions). Because dark-adapted and light-adapted eyes demonstrated the same peak spectral responses, we conclude that neither short (SWS) nor long wavelength-sensitive (LWS) photoreceptors are present in *A. heterochaelis*. We recorded narrower spectral response peaks in our light-adapted trials than in our dark-adapted trials, which suggests the presence of more than one class of MWS photoreceptor in the eyes of *A. heterochaelis*.

Our results from MSP were consistent with our results from ERG and revealed the presence of at least two MWS photoreceptors in the eyes of *A. heterochaelis*. We measured the absorption of light by 76 separate photoreceptors from n=6 individuals. We found that 62% of these photoreceptors contained a visual pigment with a wavelength of peak absorption (λ_{max}) of 500±3 nm (Fig. 5, black

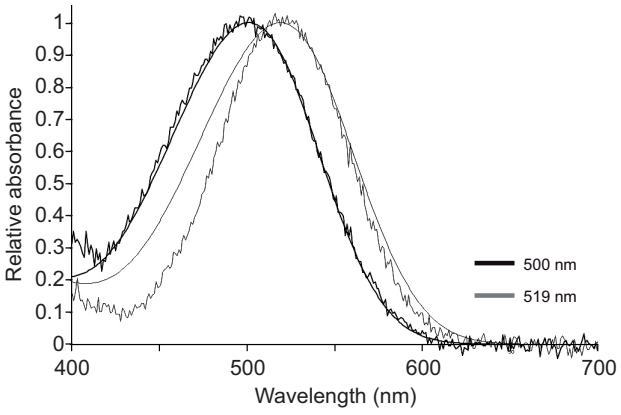

Fig. 5. Relative absorbance of visual pigments in the eyes of *A. heterochaelis* assessed by microspectrophotometry (MSP). Averaged absorbance of 47 visual pigments where the best-fit λ_{max}=501 nm (black line) and of 29 visual pigments where the best-fit λ_{max}=519 nm (gray line). Both classes of visual pigments were fitted to a standard Govardovskii et al. (2000) rhodopsin template (smooth black and gray lines).

Journal of Experimental Biology (2019) 222, jeb209015. doi:10.1242/jeb.209015

trace). In 38% of these photoreceptors, we found visual pigments with λ_{max} values that ranged from 510 to 527 nm with an average λ_{max} of 519±5 nm (Fig. 5, gray trace). These two classes of MWS photoreceptors appeared to be distributed similarly across the eyes and did not appear to differ morphologically.

Snapping shrimp demonstrate a rapid rate of temporal sampling

Using ERG, we found the eyes of *A. heterochaelis* have a FFF of at least 41 Hz when tested using a 500 nm stimulus at an intensity of 7.89×10^{14} photons cm^{-2} s^{-1} (Fig. 6). The FFF for the animals we tested was 41±7 Hz, with a range of 32 to 49 Hz. We did not test frequencies over 49 Hz because this was the highest frequency at which we could operate the shutter given the configuration of our system. Because we did not adjust the intensity of the stimulus during these trials, we did not measure the critical flicker fusion frequency (cFFF) of *A. heterochaelis*. Thus, it is likely that our measurement of FFF underestimates the cFFF of this species.

Behavioral evidence for spatial vision in snapping shrimp

Behavioral tests indicated the eyes of snapping shrimp provide spatial vision with an angular resolution of ~8 deg (Fig. 7). In the first set of trials (n=33), 27 animals followed moving stripes with angular widths of 20 deg, 23 followed the 15 deg stripes, and 16 followed the 10 deg stripes (P<0.0001 for each stimulus). In the second set of trials (n=23), 12 animals followed moving stripes with angular widths of 12 deg, 11 followed the 8 deg stripes, and 8 followed the 4 deg stripes (P<0.0001, P=0.0002 and P=0.0038, respectively). In the third set of trials (n=30), 10 animals followed moving stripes with angular widths of 4 deg, 5 followed the 2 deg stripes, 3 followed the 1 deg stripes and 3 followed the 0.5 deg stripes (P=0.0056, P=0.1945, P=0.6120 and P=0.6120, respectively). Across all three sets of trials, only 1 out of 86 animals followed the control stimulus. Using Fisher's exact test, while correcting for multiple comparisons, we found *A. heterochaelis* followed moving stripes 4 deg or wider but did not follow stripes narrower than 4 deg. As a measure of spatial resolution, we estimated minimum resolvable angle (α_{min}) in *A. heterochaelis* to be 8 deg, twice the width of the narrowest stripes that it followed (4 deg).

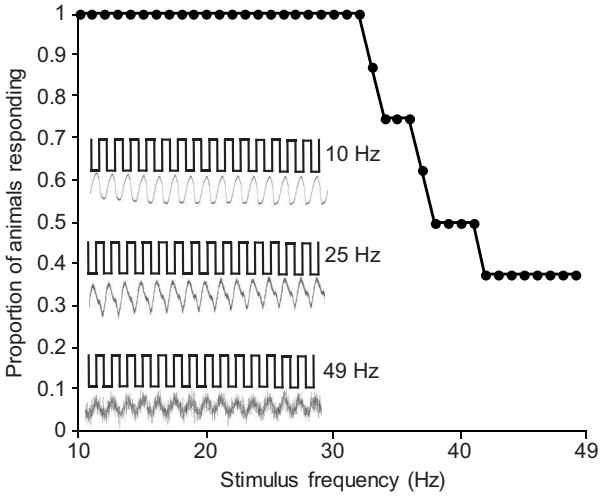

Fig. 6. Temporal sampling rates of *A. heterochaelis* assessed by extracellular ERG from 10 to 49 Hz. Data are the proportion of animals that responded to a light stimulus flickering at the rate indicated (flicker fusion frequency, FFF) (n=8). Inset: representative ERG recordings at 10, 25 and 49 Hz where the upper trace is the flickering stimulus and the lower trace is the corresponding electrophysiological response of an *A. heterochaelis* eye.

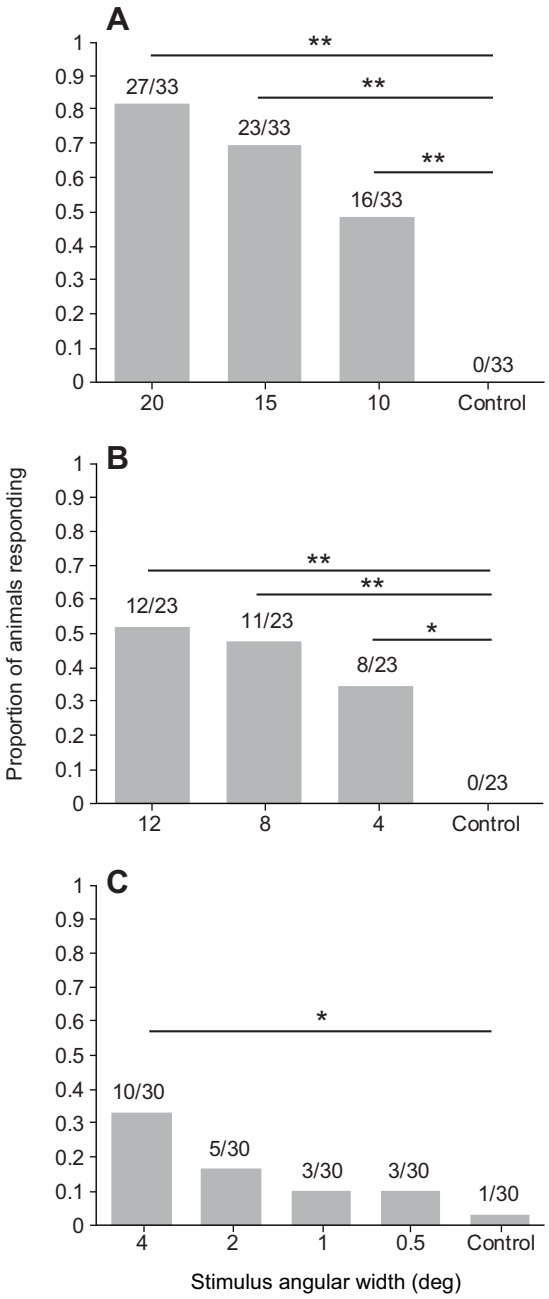

Fig. 7. Responses of *A. heterochaelis* in three sets of optomotor behavioral trials. (A) In the first set of trials, the test stimuli had angular widths of 20, 15 or 10 deg. (B) In the second set of trials, the test stimuli had angular widths of 12, 8 or 4 deg. (C) In the third set of trials, the test stimuli had angular widths of 4, 2, 1 or 0.5 deg. Test stimuli were black and white stripes of equal width and the control stimulus was a uniform 50% gray. The numbers above the bars represent the number of animals that followed each stimulus out of the total number of animals tested. *P<0.05 and **P<0.01 following Bonferroni correction.

DISCUSSION

Characterizing the visual abilities of *A. heterochaelis*

Using morphological, physiological and behavioral approaches, we have demonstrated for the first time that the eyes of snapping shrimp provide spatial vision. Beneath their highly transparent orbital

hoods, *A. heterochaelis* have compound eyes with reflecting superposition optics. Based on their morphology, we estimate the eyes of *A. heterochaelis* provide an angular resolution ($\Delta\phi$) of 6 deg, which falls within the range of angular resolutions (<1 to 11.3 deg) estimated for the reflecting superposition eyes of other decapods (Berón de Astrada et al., 2012; Dobson et al., 2014; Smolka and Hemmi, 2009). Our behavioral estimate of spatial acuity (α_{min}) of 8 deg is consistent with both our morphological estimate of angular resolution in *A. heterochaelis* and behavioral estimates of spatial acuity in other decapods. Blue crabs and cleaner shrimp, for example, demonstrate α_{min} values of 2 and 8–11 deg, respectively (Baldwin and Johnsen, 2011; Caves et al., 2016). Angular resolution in *A. heterochaelis* may be context dependent as a result of spatial summation (Cronin et al., 2014), so we do not suggest 8 deg as the exact angular resolution of *A. heterochaelis*. However, we are confident that snapping shrimp demonstrate spatial vision and that their visual abilities are not inferior to those of similarly sized decapods from shallow marine habitats.

Like other shallow-dwelling decapods (Cronin, 2006; Goldsmith and Fernandez, 1968; Johnson et al., 2002; Marshall et al., 1999, 2003), we found that *A. heterochaelis* is maximally sensitive to the blue–green wavelengths prevalent in coastal marine habitats (Jerlov, 1976; Tyler and Smith, 1970). Further, our results suggest that *A. heterochaelis* has at least two MWS photoreceptors with peak spectral responses at 500 and 519 nm. We think it unlikely that SWS or LWS photoreceptors are present in the eyes of *A. heterochaelis*, but we cannot rule out the presence of UV-sensitive (UVS) photoreceptors. Many decapods have UV-sensitive R8 cells and although we did not find morphological evidence of R8 cells in the eyes of *A. heterochaelis*, we did not test for UV sensitivity using ERG or MSP.

Compared with the eyes of other decapods, those of *A. heterochaelis* demonstrate a high rate of temporal sampling. Temporal sampling rates in decapods range from 20 to 60 Hz (Caves et al., 2016; Meyer-Rochow, 2001), with the eyes of *A. heterochaelis* performing in the upper part of this range (FFF>40 Hz). A high temporal sampling rate may be related to the high speed at which snapping shrimp move. These animals move quickly across the substrate and snap frequently during interactions with conspecifics, predators and prey. We hypothesize that a high rate of temporal sampling may help snapping shrimp to avoid the snaps of conspecifics during agonistic interactions and to accurately aim their snaps at fast-moving targets.

Reassessing the visual ecology of snapping shrimp

Demonstrating spatial vision in *A. heterochaelis* prompts a re-evaluation of the behavioral associations between snapping shrimp and their heterospecific partners. Previous authors have argued that these associations occur because the orbital hoods of snapping shrimp obscure their eyes, rendering them blind and in need of aid from other species, such as gobies, to help them avoid predators (Luther, 1958; Magnus, 1967). Our discovery that orbital hoods do not preclude spatial vision in *A. heterochaelis*, a species that does not engage in heterospecific behavioral associations, suggests other species of snapping shrimp have spatial vision too, including those that engage in heterospecific behavioral associations. Orbital hood morphology differs considerably across species of snapping shrimp, but it differs little across species of *Alpheus* (Anker et al., 2006). All snapping shrimp known to have behavioral associations with gobies are species of *Alpheus* (Karplus, 1987), so our work suggests that a lack of spatial vision does not explain why some species of snapping shrimp form partnerships with gobies.

To explain the heterospecific behavioral associations of snapping shrimp, we propose a division-of-labor model for tasks performed by snapping shrimp and their partners. The eyes of gobies almost certainly provide finer spatial acuity than those of snapping shrimp, so gobies may be better able to detect approaching predators than snapping shrimp. In exchange, snapping shrimp provide housing and protection to their goby partners, as they are industrious burrowers with potentially lethal weapons.

Our results raise the possibility that snapping shrimp use visual cues to communicate with heterospecific partners and conspecifics. Although snapping shrimp may remain in continual physical contact with their goby partners (Magnus, 1967; Preston, 1978), we hypothesize that snapping shrimp and their partners may also communicate visually. For example, snapping shrimp may use vision to assess individual gobies as potential partners. Movements by goby partners in response to approaching predators may also be detected visually by snapping shrimp (Preston, 1978). Our work also supports previous findings that snapping shrimp use visual assessment of claw size to evaluate conspecifics during agonistic interactions (Hughes, 1996a,b).

Lastly, establishing that *A. heterochaelis* has spatial vision leads to new questions about how the orbital hoods, visual abilities and behavioral associations of snapping shrimp may have co-evolved. For example, the orbital hoods of snapping shrimp have a higher refractive index than seawater, so they may contribute to vision by acting as a refractive surface. Orbital hoods may also protect the heads of snapping shrimp from the shock waves produced by their own claws (Anker et al., 2006). Snapping shrimp engage frequently in agonistic interactions (Schmitz and Herberholz, 1998), and we hypothesize that orbital hoods may also protect against damage from conspecifics snapping at close range.

Acknowledgements

We thank Dan Chappell, Jamie Clark, Natalie Sanchez and David Kingston for help collecting snapping shrimp. For help designing our optomotor apparatus we thank Olivia Harris and Jeff Dudycha. We thank the Baruch Institute and the Baruch Marine Field Laboratory for access to collecting sites and for use of their facilities. We are particularly grateful to Dennis Allen for his wisdom and guidance in collecting snapping shrimp.

Competing interests

The authors declare no competing or financial interests.

Author contributions

Conceptualization: A.C.N.K., D.I.S.; Methodology: A.C.N.K., L.T.H., T.W.C., D.I.S.; Software: L.T.H.; Validation: A.C.N.K., L.T.H.; Formal analysis: A.C.N.K., L.T.H., T.W.C.; Investigation: A.C.N.K., R.L.L.; Resources: A.C.N.K., T.W.C., D.I.S.; Writing - original draft: A.C.N.K., D.I.S.; Writing - review and editing: A.C.N.K., R.L.L., L.T.H., T.W.C., D.I.S.; Visualization: A.C.N.K.; Supervision: A.C.N.K., D.I.S.; Project administration: A.C.N.K., D.I.S.; Funding acquisition: A.C.N.K., D.I.S.

Funding

This research was supported, in part, by a Baruch Foundation 2017 Visiting Scientist Award (to A.C.N.K.), University of South Carolina ASPIRE Track IIB (to A.C.N.K.), and IOS Award no. 1457148 from the National Science Foundation (to D.I.S.).

Supplementary information

Supplementary information available online at
http://jeb.biologists.org/lookup/doi/10.1242/jeb.209015.supplemental

References

Anker, A., Ahyong, S. T., Noel, P. Y. and Palmer, A. R. (2006). Morphological phylogeny of alpheid shrimps: parallel preadaptation and the origin of a key morphological innovation, the snapping claw. *Evolution* **60**, 2507-2528. doi:10.1111/j.0014-3820.2006.tb01886.x

Baldwin, J. and Johnsen, S. (2011). Effects of molting on the visual acuity of the blue crab, *Callinectes sapidus*. *J. Exp. Biol.* **214**, 3055-3061. doi:10.1242/jeb.056861

Bechstedt, S., Lu, K. and Brouhard, G. J. (2014). Doublecortin recognizes the longitudinal curvature of the microtubule end and lattice. *Curr. Biol.* **24**, 2366-2375. doi:10.1016/j.cub.2014.08.039
Becking, L. B. and Chamberlin, J. C. (1925). A note on the refractive index of chitin. *Proc. Soc. Exp. Biol. Med.* **22**, 256-256. doi:10.3181/00379727-22-120
Berón de Astrada, M., Bengochea, M., Medan, V. and Tomsic, D. (2012). Regionalization in the eye of the grapsid crab *Neohelice granulata* (=*Chasmagnathus granulatus*): variation of resolution and facet diameters. *J. Comp. Physiol. A* **198**, 173-180. doi:10.1007/s00359-011-0697-7
Caves, E. M., Frank, T. M. and Johnsen, S. (2016). Spectral sensitivity, spatial resolution and temporal resolution and their implications for conspecific signalling in cleaner shrimp. *J. Exp. Biol.* **219**, 597-608. doi:10.1242/jeb.122275
Cronin, T. W. (2006). Invertebrate vision in water. In *Invertebrate Vision* (ed. E. Warrant and D.-E. Nilsson), pp. 211-249. Cambridge: Cambridge University Press.
Cronin, T. W. and Forward, R. B., Jr (1988). The visual pigments of crabs. *J. Comp. Physiol. A* **162**, 463-478. doi:10.1007/BF00612512
Cronin, T. W. and Marshall, N. J. (1989). A retina with at least ten spectral types of photoreceptors in a mantis shrimp. *Nature* **339**, 137-140. doi:10.1038/339137a0
Cronin, T., Caldwell, R. and Erdmann, M. (2002). Tuning of photoreceptor function in three mantis shrimp species that inhabit a range of depths. I. Visual pigments. *J. Comp. Physiol. A* **188**, 179-186. doi:10.1007/s00359-002-0291-0
Cronin, T. W., Johnsen, S., Marshall, N. J. and Warrant, E. J. (2014). *Visual Ecology*. Princeton: Princeton University Press.
Dobson, N. C., De Grave, S. and Johnson, M. L. (2014). Linking eye design with host symbiont relationships in pontoniine shrimps (Crustacea, Decapoda, Palaemonidae). *PLoS ONE* **9**, e99505. doi:10.1371/journal.pone.0099505
Frank, T. M., Johnsen, S. and Cronin, T. W. (2012). Light and vision in the deep-sea benthos: II. Vision in deep-sea crustaceans. *J. Exp. Biol.* **215**, 3344-3353. doi:10.1242/jeb.072033
Goldsmith, T. H. and Fernandez, H. R. (1968). Comparative studies of crustacean spectral sensitivity. *Zeitschrift für vergleichende Physiologie* **60**, 156-175. doi:10.1007/BF00878449
Govardovskii, V. I., Fyhrquist, N., Reuter, T., Kuzmin, D. G. and Donner, K. (2000). In search of the visual pigment template. *Vis. Neurosci.* **17**, 509-528. doi:10.1017/S0952523800174036
Hathaway, C. R. and Dudycha, J. L. (2018). Quantitative measurement of the optomotor response in free-swimming Daphnia. *J. Plankton Res.* **40**, 222-229. doi:10.1093/plankt/fby014
Hughes, M. (1996a). The function of concurrent signals: visual and chemical communication in snapping shrimp. *Anim. Behav.* **52**, 247-257. doi:10.1006/anbe.1996.0170
Hughes, M. (1996b). Size assessment via a visual signal in snapping shrimp. *Behav. Ecol. Sociobiol.* **38**, 51-57. doi:10.1007/s002650050216
Jerlov, N. G. (1976). *Marine Optics*, 2nd edn. Amsterdam: Elsivier Science.
Johnson, M. L., Gaten, E. and Shelton, P. M. J. (2002). Spectral sensitivities of five marine decapod crustaceans and a review of spectral sensitivity variation in relation to habitat. *J. Mar. Biol. Assoc. U. K.* **82**, 835-842. doi:10.1017/S0025315402006203
Karplus, I. (1987). The association between gobiid fishes and burrowing alpheid shrimps. *Oceanogr. Mar. Biol.* **25**, 507-562.
Karplus, I. and Thompson, A. R. (2011). The partnership between gobiid fishes and burrowing alpheid shrimps. In *The Biology of Gobies* (ed. R. A. Patzner, J. L. Van Tassell, M. Kovacic and B. G. Kapoor), pp. 559-608. Boca Raton: Science.
Knowlton, R. E. and Moulton, J. M. (1963). Sound production in the snapping shrimps *Alpheus* (Crangon) and *Synalpheus*. *Biol. Bull.* **125**, 311-331. doi:10.2307/1539406
Land, M. F. and Nilsson, D.-E. (2012). *Animal Eyes* (ed. P. Willmer and D. Norman). Oxford: Oxford University Press.
Lohse, D., Schmitz, B. and Versluis, M. (2001). Snapping shrimp make flashing bubbles. *Nature* **413**, 1-2. doi:10.1038/35097152
Luther, V. W. (1958). Symbiose von Fischen (Gobiidae) mit einem Krebs (*Alpheus djiboutensis*) im Roten Meer. *Aus dem Zoologischen Institut der Technischen Hochschule, Darmstadt* **15**, 175-177.
Magnus, D. B. E. (1967). Zur Ökologie sedimentbewohnender *Alpheus*-Garnelen (Decapoda, Natantia) des Roten Meeres. *Heloglander Wissenschaftliches Meeresuntersuchungen* **15**, 506-522. doi:10.1007/BF01618647
Marshall, J., Kent, J. and Cronin, T. W. (1999). Visual adaptations in crustaceans: spectral sensitivity in diverse habitats. In *Adaptive Mechanisms in the Ecology of Vision* (ed. S. N. Archer, M. B. A. Djamgoz, E. R. Loew, J. C. Partridge and S. Vallerga), pp. 285-327. Dordrecht: Kluwer Academic Publishers.
Marshall, N. J., Cronin, T. W. and Frank, T. M. (2003). Visual adaptations in crustaceans: chromatic, developmental, and temporal aspects. In *Sensory Processing in Aquatic Environments* (ed. S. P. Collin and N. J. Marshall), pp. 343-372. New York: Springer.
McCann, G. D. and MacGinitie, G. F. (1965). Optomotor response studies of insect vision. *Proc. R. Soc. B* **163**, 369-401. doi:10.1098/rspb.1965.0074
Melzer, R. R., Diersch, R., Nicastro, D. and Smola, U. (1997). Compound eye evolution: Highly conserved retinula and cone cell patterns indicate a common origin of the insect and crustacean ommatidium. *Naturwissenschaften* **84**, 542-544. doi:10.1007/s001140050442
Meyer-Rochow, V. B. (2001). The crustacean eye: dark/light adaptation, polarization sensitivity, flicker fusion frequency, and photoreceptor damage. *Zoolog. Sci.* **18**, 1175-1197. doi:10.2108/zsj.18.1175
Preston, J. L. (1978). Communication systems and social interactions in a goby-shrimp symbiosis. *Anim. Behav.* **26**, 791-802. doi:10.1016/0003-3472(78)90144-6
Schindelin, J., Arganda-Carreras, I., Frise, E., Kaynig, V., Longair, M., Pietzsch, T., Preibisch, S., Rueden, C., Saalfeld, S., Schmid, B. et al. (2012). Fiji: an open-source platform for biological-image analysis. *Nat. Methods* **9**, 676-682. doi:10.1038/nmeth.2019
Schmitz, B. and Herberholz, J. (1998). Snapping behaviour in intraspecific agonistic encounters in the snapping shrimp (*Alpheus heterchaelis*). *J. Biosci.* **23**, 623-632. doi:10.1007/BF02709175
Smolka, J. and Hemmi, J. M. (2009). Topography of vision and behaviour. *J. Exp. Biol.* **212**, 3522-3532. doi:10.1242/jeb.032359
Tyler, J. E. and Smith, R. C. (1970). *Measurements of Spectral Irradiance Underwater*. New York: Gordon and Breach.
Versluis, M., Schmitz, B., von der Heydt, A. and Lohse, D. (2000). How snapping shrimp snap: through cavitating bubbles. *Science* **289**, 2114-2117. doi:10.1126/science.289.5487.2114

Movie 1. Behavioral evidence for spatial vision in snapping shrimp. In this representative movie, a snapping shrimp (*A. heterochaelis*) is seen following moving stripes with angular widths of 20°. When the stimulus changes direction, the shrimp also changes direction to follow the stimulus. This video is a subsample of the full-length video.